Glycobiology vol. 10 no. 1 pp. 89–101, 2000

Schistosoma mansoni cercarial glycolipids are dominated by Lewis X and pseudo-Lewis Y structures

Manfred Wuhrer, Roger D.Dennis, Michael J.Doenhoff[2], Günter Lochnit and Rudolf Geyer[1]

Institute of Biochemistry, University of Giessen, D-35392 Giessen, Germany, and [2]School of Biological Sciences, University of Wales, Bangor, Wales LL57 2UW, UK

Received on May 6, 1999; revised on May 19, 1999; accepted on May 23, 1999

The oligosaccharide structures of glycolipids from cercariae of the human blood fluke, *Schistosoma mansoni*, were analyzed in the form of their corresponding, pyridylaminated oligosaccharides by methylation analysis, partial hydrolysis, exoglycosidase treatment, on-target exoglycosidase cleavage and matrix-assisted laser desorption/ionization time-of-flight mass spectrometry. The six, dominant chemical structures present have been determined as: GalNAc(β1–4)Glc1-ceramide; GlcNAc(β1–3)GalNAc(β1–4)Glc1-ceramide; Gal(β1–4)GlcNAc(β1–3)GalNAc(β1–4)Glc1-ceramide; Gal(β1–4)[Fuc(α1–3)]GlcNAc(β1–3)GalNAc(β1–4)Glc1-ceramide (Lewis X pentasaccharide structure); Gal(β1–4)[Fuc(α1–3)]GlcNAc(β1–3)GlcNAc(β1–3)GalNAc(β1–4)Glc1-ceramide (Lewis X hexasaccharide structure); and, Fuc(α1–3)Gal(β1–4)[Fuc(α1–3)]GlcNAc(β1–3)GalNAc(β1–4)Glc1-ceramide (pseudo-Lewis Y hexasaccharide structure). These structures belong to the characterized schisto-series of protostomial glycosphingolipids. The Lewis X and pseudo-Lewis Y glycolipids are stage-specifically expressed by the cercarial life-cycle stage, and not by the adult or egg.

Key words: CD15/oligosaccharide structural analysis/on-target enzymatic cleavage/*Schistosoma mansoni* antigenic glycolipids/stage-specific expression

Introduction

Schistosomes express a variety of different carbohydrate structures (Cummings and Nyame, 1996), several of which give rise to a strong humoral response during infection. Some of these carbohydrate antigens have been found to be restricted to this parasite (Nyame *et al.*, 1989; Srivatsan *et al.*, 1992b; Bergwerff *et al.*, 1994; Khoo *et al.*, 1995; Mansour, 1996; Negm, 1996; Khoo *et al.*, 1997). In addition, the unique glycosylation patterns common to schistosomal proteins and glycolipids have been found to differ structurally and immunologically from all other glycolipids detected so far in the animal kingdom. Makaaru *et al.* (1992) have shown *Schistosoma mansoni* glycolipids to have an *N*-acetylgalactosamine residue in the second position of the carbohydrate chain. *S.mansoni* glycolipids have been found to be highly antigenic (Weiss *et al.*, 1986) and adult *S.mansoni* glycolipids to be potentially useful antigens for the serodiagnosis of schistosomiasis (Dennis *et al.*, 1996), due to the high titers of antibodies reacting with them in chronic infection sera and the absence of significant cross-reactivity with other helminth infection sera. The major epitope present on glycolipids from adults, cercariae, and eggs was also shown to be present on egg glycoproteins (Weiss and Strand, 1985). Structural analysis of egg stage antigenic glycolipids has revealed large, branched glycans with oligofucosyl side-chains on an *N*-acetylhexosamine backbone built up by the repetitive unit –4[±Fucα2Fucα3]GlcNAcβ- and the chain-termination motif of ±Fucα2Fucα3GalNAcβ- (Khoo *et al.*, 1997). Indication for a second schistosomal glycolipid epitope was given by the immunostaining of high-performance thin-layer chromatography (HPTLC)-separated glycolipids with a monoclonal antibody (mAb) that gave a weak recognition signal with cercarial stage glycolipids only (Weiss *et al.*, 1986). This mAb was later found to be specific for Lewis X (Le^x) and binds to the tegument and gut of *S.mansoni* adults, to the acetabular gland opening of cercariae and to schistosomula obtained by *in vitro* transformation (Dalton *et al.*, 1987; Köster and Strand, 1994). Le^x, also termed CD15 or SSEA I (stage-specific embryonic antigen I), is shared between the parasite and the mammalian host (Ko *et al.*, 1990; Nyame *et al.*, 1998), and during infection a humoral immune response to this epitope, classified as autoimmune, has been observed (Nyame *et al.*, 1995, 1996, 1997). These results obtained by immunological techniques paralleled structural analyses detecting Le^x on adult worm glycoproteins (Srivatsan *et al.*, 1992a) as well as on the circulating cathodic antigen (van Dam *et al.*, 1994), which is assumed to be secreted from the adult parasite gut (Deelder and Kornelis, 1980).

The aim of this study was to structurally analyze the oligosaccharide chains present in the biosynthetic series of neutral glycolipids from cercariae, the stage-specific expression of Le^x-containing glycolipids in cercariae and to compare the pattern of cercarial glycolipid structures identified with those present in *S.mansoni* eggs.

Results

Isolation and immunochemical characterization

Glycolipids isolated from the *S.mansoni* life-cycle stages were fractionated on a silica gel cartridge. The complex glycolipid fractions of adults, cercariae and eggs were all recognized by

[1]To whom correspondence should be addressed at: Biochemisches Institut am Klinikum der Universität, Friedrichstrasse 24, D-35392 Giessen, Germany

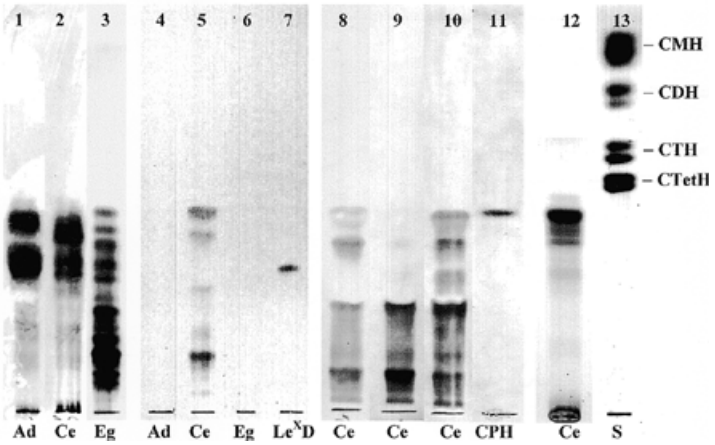

Fig. 1. HPTLC-immunostaining of *S.mansoni* glycolipids. Aliquots of adult, cercarial and egg complex glycolipid fractions were developed with chloroform/methanol/0.25% KCl (50:40:10, by volume). The amount of glycolipid extract applied in lanes 1–6 corresponded to 500, 50 and 5 μg of lyophilized parasite material for adults (Ad), cercariae (Ce) and eggs (Eg), respectively. A Le^x-neoglycolipid (Le^xD; 400 ng carbohydrate) was used as positive control (lane 7). In lanes 8–10, amounts of cercarial complex glycolipid fraction corresponded to 500 μg of lyophilized cercariae. 20 ng of the purified ceramide pentahexoside (CPH) was used in lane 11. Glycolipids were visualized by immunostaining in lanes 1–3 with a pool of 8 *S.mansoni* chronic infection sera, diluted 1:500; in lanes 4–8 with mAb BRA4F1, 1:200; in lane 9 with mAb 4D1, 1:200; in lanes 10 and 11 with mAb G8G12, 1:500. Cercarial complex glycolipid fraction (lane 12; corresponding to 10 mg of lyophilized cercariae) and globoside standard (S; lane 13) were visualized with orcinol/H_2SO_4.

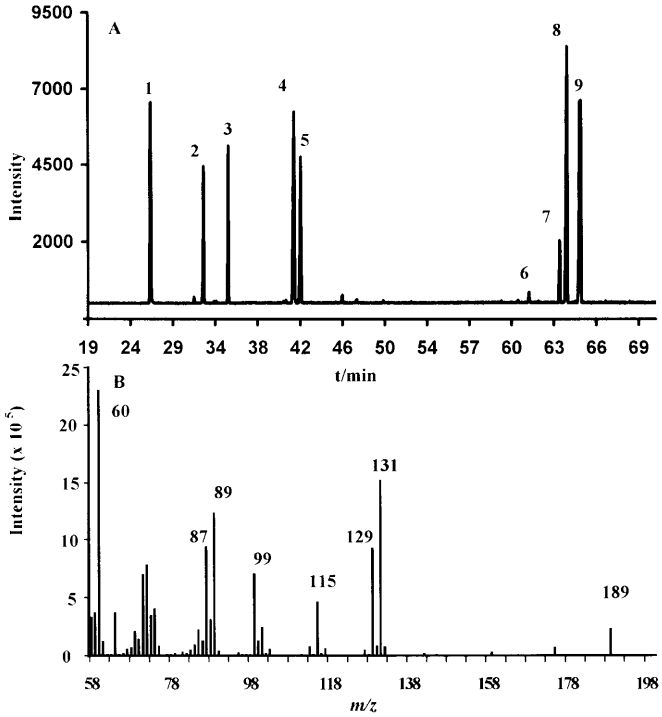

Fig. 2. Methylation analysis of the cercarial complex glycolipid fraction. The partially methylated sugar derivatives obtained after permethylation, hydrolysis, reduction and peracetylation were analyzed by capillary GC/MS (DB1- and DB210-columns; Macherey & Nagel). (**A**) Total ion chromatogram with chemical ionisation (DB1-column, 60 m). 1: 2,3,4-FucOH, (2,3,4-tri-*O*-methylfucitol); 2: 3,4-FucOH; 3: 2,3,4,6-GalOH; 4: 2,3,6-GlcOH; 5: 2,4,6-GalOH; 6: 3,6-GlcN(Me)AcOH (2-deoxy-2-(*N*-methyl)acetamido-3,6-di-*O*-methylglucitol); 7: 4,6-GlcN(Me)AcOH; 8: 3,6-GalN(Me)AcOH; 9: 6-GlcN(Me)AcOH. (**B**) Mass spectrum of the 3,4-FucOH component (peak 2 in **A**) after electron impact ionization.

chronic infection sera (Figure 1, lanes 1–3), but the Le^x-epitope was only detected on cercarial glycolipids (Figure 1, lane 5) and not on adult or egg glycolipids (Figure 1, lanes 4 and 6), as shown by HPTLC-immunostaining with the mouse mAb anti-CD15 BRA4F1. Two other anti-Le^x mAbs also showed a stage-specific recognition of several cercarial, but not adult or egg glycolipids (data not shown). These three anti-Le^x mAbs differed in their recognition patterns of cercarial glycolipids (Figure 1, lanes 8–10). The smallest species recognized exhibited migration properties of a ceramide pentahexoside (CPH; Figure 1, lane 11) and reacted strongly with the mAb G8G12, weakly with the mAb anti-CD15 BRA4F1 and, under the conditions applied, only very weakly with the mouse-mAb anti-CD15 4D1. The antibodies differed in their recognition of this apparent CPH and some other, slightly larger glycolipids, but showed identical reaction with the large, slow-migrating cercarial glycolipids on HPTLC-immunostaining. Thus, the mAb G8G12 seemed to be an anti-Le^x mAb, just as the other two monoclonal antibodies applied, with the differences in recognition pattern possibly due to variability in epitopic specificities. Orcinol-staining of cercarial complex glycolipids (Figure 1, lane 12) revealed a strong signal for the putative CPH, followed by a band-doublet. A background of orcinol-positive material below this doublet indicated the presence of several minor components. While the CPH component was chemically dominant, the larger glycolipids were obviously recognized more strongly by the three mAbs used (Figure 1, lanes 8–10), i.e., immunochemically dominant. The finding that CPH is only weakly stained immunochemically by the three anti-Le^x mAbs applied agrees with reports that most of the mAbs recognizing Le^x-glycolipids are less reactive with CPH comprising the Le^x-epitope than, for example, ceramide heptahexoside species (Umeda *et al.*, 1986).

Linkage analysis of the complex glycolipid fraction

Methylation analysis of the cercarial complex glycolipid fraction revealed fucose to be either terminal or monosubstituted (an internal residue; Figure 2A). The monosubstituted fucose was further analyzed by gas chromatography/mass spectrometry (GC/MS) in the electron impact mode (Figure 2B). Comparison of the fragmentation pattern to published data (Hellerqvist, 1990) and to a spectrum deposited in a data base (Carbbank, Complex Carbohydrate Research Center, Athens, GA) revealed the fucose to be 2-substituted (1,2,5-tri-*O*-acetyl-3,4-di-*O*-methylfucitol).

Structural analysis of intact glycolipids

Purified, cercarial glycolipids were fractionated by Iatrobeads HPLC. Fractions, visualized by HPTLC and orcinol/H_2SO_4-staining (data not shown), were pooled to yield ceramide dihexoside (CDH) and CPH. Matrix-assisted laser desorption/ionization time-of-flight mass spectrometry (MALDI-TOF-MS) revealed an identical pattern of ceramide heterogeneity

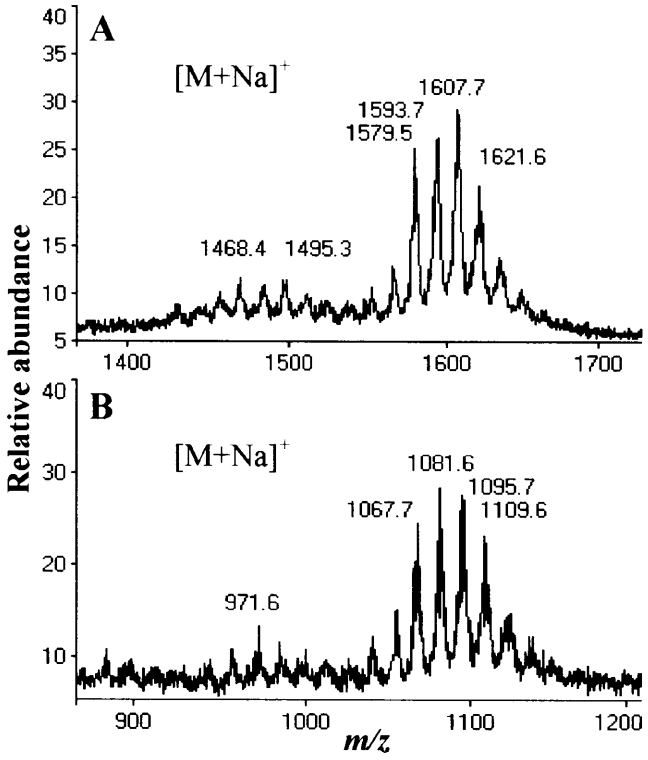

Fig. 3. Analysis of ceramide pentahexoside (CPH; **A**) and ceramide dihexoside (CDH; **B**) by MALDI-TOF-MS illustrating the identical pattern in ceramide heterogeneity.

for the two glycolipids (Figure 3). While complex egg glycolipids mainly possessed a ceramide moiety of a t20:0 sphingoid base and C16:0 fatty acid (Khoo *et al.*, 1997), the corresponding cercarial-stage CDH-species at *m/z* 971.6 was only a minor component (Figure 3B). Cercarial CDH and complex glycolipids, as exemplified by CPH (Figure 3A), were dominated by ceramides of more that 40 carbon atoms, which have not been further analyzed in this study. The CPH component analyzed by composition (Table III) and linkage analyzes (Table IV) was found to contain the Le^x-epitope by HPTLC-immunostaining and to be identical to the fastest-migrating, chromatographic band of cercarial complex glycolipids recognized by the mAb G8G12 (Figure 1, lane 11).

Preparation and separation of PA-oligosaccharides

In order to study individual oligosaccharides, glycans were released from the ceramide moiety by endoglycoceramidase treatment of an aliquot of the cercarial complex glycolipid fraction. For the separation of uncleaved glycolipids and ceramides from the released oligosaccharides, the sample was fractionated on a reverse phase (RP)-cartridge. Released oligosaccharides were collected as the combined flow-through and wash fractions, while the uncleaved glycolipids were obtained by elution with organic solvents. Released glycans and uncleaved glycolipids were quantitated by composition analysis (Table I), showing an average efficacy of over 80% glycan release for the different monosaccharides. The released oligosaccharides were pooled and labeled with the fluorescent tag, 2-aminopyridine (PA). PA-oligosaccharides were fractionated by amino-phase high-performance liquid chromatography (HPLC; Figure 4). Collected fractions (***1*** to ***17***; thereafter, fractions denoted by number only) were screened by MALDI-TOF-MS and assessed for monosaccharide content by composition analysis (Tables II and III). Fractions ***1*** to ***5*** were found not to contain carbohydrate and the major component turned out to be the PA-pentasaccharide ***12***. In order to reduce peak heterogeneity and obtain as far as possible pure compounds, several of the amino-phase fractions were subfractionated by RP-HPLC. Subfractions (designated, for example, ***6-1*** for subfraction ***1*** of fraction ***6***) were again screened by MALDI-TOF-MS and composition analysis (Tables II and III). From the measured pseudomolecular ions, the compositions of the PA-oligosaccharides could be deduced (Table II). The PA-disaccharide ***6-1***, the PA-trisaccharide ***8-5***, and the PA-hexasaccharides ***13-2*** and ***14-3*** thus obtained were the major components of the fractions 6, 8, 13, and 14, respectively. Together with the PA-pentasaccharide ***12***, these were the major components determined and the data provided here allowed a detailed, structural characterization of these components.

Table I. Efficacy of endoglycoceramidase cleavage of the cercarial complex glycolipid fraction shown by composition analysis

Monosaccharide	Cercarial glycolipid fraction	Released monosaccharide (μg)		Released monosaccharide (%)
		Water fraction	Organic solvent fraction	
GalN	(1.0)	147 (1.0)	21 (1.0)	88
GlcN	(1.3)	127 (0.9)	33 (1.6)	79
Gal	(1.0)	165 (1.1)	42 (2.0)	79
Man	(0.1)		16 (0.8)	—
Glc	(0.5)	176 (1.2)	68 (3.2)	72
Fuc	(2.6)	294 (2.0)	46 (2.2)	87

Cercarial complex glycolipids were cleaved with endoglycoceramidase and fractionated on a RP-cartridge. The aqueous fractions of two experiments were combined (water fraction) as well as the organic solvent-eluted fractions (organic solvent fraction) and compared by composition analysis to the starting cercarial complex glycolipid fraction. The amounts of monosaccharides are given in micrograms and their relative ratios are given with GalN = 1.0 in parentheses. GalN, galactosamine; GlcN, glucosamine.

Table II. Analysis of PA-oligosaccharides by MALDI-TOF-MS

Fraction	Measured mass [Adduct] (Theoretical mass)	Composition
6-1	468.3 $[M+Li]^+$ (468.2); 462.2 $[M+H]^+$ (462.2)	Hex HexNAc PA
8-5	671.3 $[M+Li]^+$ (671.3); 665.3 $[M+H]^+$ (665.3)	Hex $HexNAc_2$ PA
9-5	1020.4 $[M+Li]^+$ (1020.4); 1036.3 $[M+Na]^+$ (1036.4)	Hex $HexNAc_3$ dHex PA
10-2	833.4 $[M+Li]^+$ (833.3); 849.4 $[M+Na]^+$ (849.3)	Hex_2 $HexNAc_2$ PA
10-2-Gal	687.4 $[M+Na]^+$ (687.3); 703.3 $[M+K]^+$ (703.3)	Hex $HexNAc_2$ PA
12	979.4 $[M+Li]^+$ (979.4); 1011.2 $[M+K]^+$ (1011.4)	Hex_2 $HexNAc_2$ dHex PA
12-Fuc	833.7 $[M+Li]^+$ (833.3); 827.3 $[M+H]^+$] (827.3)	Hex_2 $HexNAc_2$ PA
12-Fuc-Gal	671.8 $[M+Li]^+$ (671.3); 687.7 $[M+Na]^+$ (687.3)	Hex $HexNAc_2$ PA
13-1	1166.5 $[M+Li]^+$ (1166.5); 1182.4 $[M+Na]^+$ (1182.5)	Hex $HexNAc_3$ $dHex_2$ PA
13-2	1125.6 $[M+Li]^+$ (1125.5); 1141.3 $[M+Na]^+$ (1141.5)	Hex_2 $HexNAc_2$ $dHex_2$ PA
13-2-Fuc	979.2 $[M+Li]^+$ (979.4); 995.4 $[M+Na]^+$ (995.4)	Hex_2 $HexNAc_2$ dHex PA
13-3	1458.4 $[M+Li^+]$ (1458.6)	Hex $HexNAc_3$ $dHex_4$ PA
13-3-Fuc	1182.4 $[M+Na]^+$ (1182.5); 1198.4 $[M+K]^+$ (1198.5)	Hex $HexNAc_3$ $dHex_2$ PA
14-3	1182.5 $[M+Li]^+$ (1182.5); 1198.4 $[M+Na]^+$ (1198.5)	Hex_2 $HexNAc_3$ dHex PA
14-3-Fuc	1052.2 $[M+Na]^+$ (1052.4); 1136.4 $[M+Li]^+$ (1136.5)	Hex_2 $HexNAc_3$ PA
14-3-Fuc-Gal	890.0 $[M+Na]^+$ (890.3); 906.1 $[M+K]^+$ (906.3)	Hex $HexNAc_3$ PA
15	979.8 $[M+Li^+]$ (979.4)	Hex_2 $HexNAc_2$ dHex PA
	1182.5 $[M+Li^+]$ (1182.4)	Hex_2 $HexNAc_3$ dHex PA
	1329.5 $[M+Li]^+$ (1328.5); 1344.8 $[M+Na]^+$ (1344.5)	Hex_2 $HexNAc_3$ $dHex_2$ PA
	1370.5 $[M+Li]^+$ (1369.6); 1402.5 $[M+K]^+$ (1401.6)	Hex $HexNAc_4$ $dHex_2$ PA
	1516.1 $[M+Li]^+$ (1515.6); 1547.7 $[M+K]^+$ (1547.6)	Hex $HexNAc_4$ $dHex_3$ PA
	1662.1 $[M+Li]^+$ (1661.7); 1693.7 $[M+K]^+$ (1693.7)	Hex $HexNAc_4$ $dHex_4$ PA
16	1491.1 $[M+Li]^+$ (1490.6)	Hex_3 $HexNAc_3$ $dHex_2$ PA
	1532.6 $[M+Li]^+$ (1531.6); 1548.3 $[M+Na]^+$ (1547.6)	Hex_2 $HexNAc_4$ $dHex_2$ PA
	1718.8 $[M+Li]^+$ (1718.7); 1735.6 $[M+Na]^+$ (1734.7)	Hex $HexNAc_5$ $dHex_3$ PA

Masses have been rounded up to the first decimal place. The type of pseudomolecular ion is given in square brackets and the calculated, monoisotopic masses in parentheses. Hex, Hexose; dHex, deoxyhexose; HexNAc, *N*-acetylhexosamine.

Table III. Composition analysis of cercarial PA-oligosaccharides and glycolipids

Fraction	Molar ratios				
	GlcN	GalN	Gal	Glc	Fuc
8-5	1.0	1.0	+	+	+
10-2	1.9	1.0	1.0	+	+
12	1.1	1.0	1.0	+	1.1
13-2	1.3	0.7	1.0	-	2.0
14-3	2.0	1.0	0.6	+	1.0
CPH	1.0	0.7	1.0	0.8	1.0

Molar ratios based on GalN = 1.0 (***8-5***, ***10-2***, ***12***, and ***14-3***) or Gal = 1.0 (***13-2*** and CPH) were determined after TFA-hydrolysis and reverse-phase chromatography of the anthranilic acid–derivatized components. The components were quantified by application of a standard mixture for determination of the individual detection response factors. GlcN, 2-amino-2-deoxy-D-glucose (glucosamine); GalN, 2-amino-2-deoxy-D-galactose (galactosamine; both monosaccharides are de-*N*-acetylated under the hydrolysis conditions applied). PA-Glc conjugates were not registered. (+), trace (<0.2).

Enzymatic and chemical hydrolysis of PA-oligosaccharides

Several of the purified PA-oligosaccharides were cleaved enzymatically and/or by partial acid hydrolysis. Enzymatic incubations were performed in ammonium acetate buffer, which allowed measurement of an aliquot of the incubated sample by MALDI-TOF-MS without further purification. Thus, the efficacy of enzymatic cleavage could easily be monitored by MALDI-TOF-MS. When cleavage was successful, the products were purified by HPLC on an amino-phase or reverse-phase column. Under the conditions of partial hydrolysis employed (0.1–0.2 M trifluoroacetic acid (TFA), 80°C, 40 to 80 min), only 10–60% of the fucose residues from PA-pentasaccharide ***12*** and PA-hexasaccharide ***14-3*** were removed. Because of this limited partial hydrolysis, fucose residues were alternatively removed by α-fucosidase treatment. One of the two terminal fucoses in the PA-hexasaccharide ***13-2*** could be removed to 80% by overnight incubation with α-fucosidase, while the second fucose present remained attached (data not shown). Similarly, PA-octasaccharide ***13-3*** could only be partially defucosylated by enzymatic treatment, in that, a 20 d-incubation with α-fucosidase produced a PA-

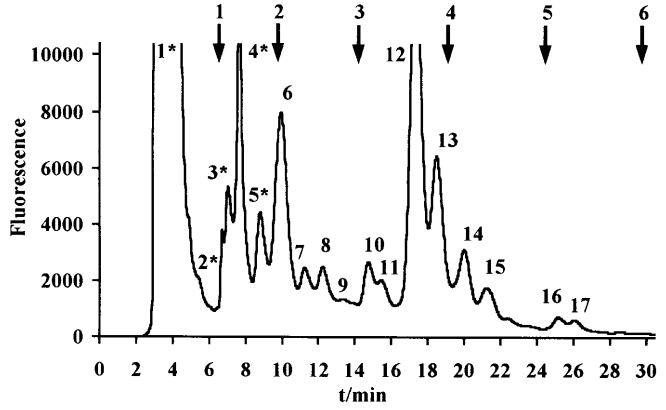

Fig. 4. HPLC separation of cercarial, glycolipid-derived PA-oligosaccharides on an amino-phase column. Elution positions of the PA-labeled dextran hydrolysate standards of different chain-length are indicated by arrows. Fractions devoid of carbohydrate-positive material are marked by asterisks (*).

hexasaccharide product with two fucose residues cleaved and two residues remaining attached (data not shown).

Quantitative defucosylation of PA-hexasaccharide ***14-3*** required a 6 d-enzymatic treatment with α-fucosidase, while a 3 d-treatment of PA-oligosaccharide ***12*** removed only 20% of the fucose residues. The chemically and enzymatically defucosylated products were pooled and designated ***12***-Fuc and ***14-3***-Fuc, respectively. The resultant PA-oligosaccharides were purified by HPLC and analyzed by MALDI-TOF-MS (Figure 5). Aliquots of ***12***-Fuc and ***14-3***-Fuc, as well as the PA-tetrasaccharide ***10-2***, were treated with β-galactosidase to achieve almost complete cleavage by overnight incubation; these samples were also HPLC-purified and designated ***12***-Fuc-Gal, ***14-3***-Fuc-Gal, and ***10-2***-Gal, respectively. The products following fucose and/or galactose removal were analyzed by MALDI-TOF-MS (Figure 5, Table II), and also for linkage (Table IV).

Linkage analysis

Glycolipids, PA-oligosaccharides, and purified cleavage products obtained after fucose and/or galactose removal were permethylated and characterized by linkage analysis (Table IV). GC/MS analysis of partially methylated alditol acetates revealed the intact cercarial CDH to contain terminal GalNAc and 4-substituted Glc (Table IV). For the corresponding PA-disaccharide (***6–1***), terminal GalNAc appeared, but the 4-substituted Glc-residue could not be determined due to its modification by reductive amination with 2-aminopyridine (Tables IV, V). All other linkage data can be interpreted on the basis of assuming a common biosynthetic series. Therefore, only changes from one oligosaccharide to the next will be named.

The PA-trisaccharide ***8-5*** has a terminal GlcNAc linked to the 3-position of subterminal GalNAc (Tables IV and V). The PA-tetrasaccharide ***10-2*** has a terminal Gal and the subterminal GlcNAc is 4-substituted. After removal of the galactose, the 4-substituted GlcNAc is converted to a terminal GlcNAc and the resulting trisaccharide ***10-2***-Gal corresponds to the structure ***8-5*** (Tables IV and V). The PA-pentasaccharide ***12*** has two terminal sugars, Fuc and Gal, while the GlcNAc is 3,4-disubstituted. The corresponding glycolipid CPH has also been isolated and, as for CDH, methylation analysis differed only in the presence of a 4-substituted Glc from the PA-oligosaccharide, which was again due to the modification of the Glc-residue in the latter compound by reductive amination with 2-aminopyridine and resultant nondetection. Methylation of ***12***-Fuc shows that the 3,4-disubstituted GlcNAc has shifted to a 4-substituted GlcNAc, which indicates Fuc to be linked to the 3-position of GlcNAc. Enzymatic cleavage to the PA-trisaccharide ***12***-Fuc-Gal converted the GlcNAc in linkage analysis to a terminal GlcNAc, thus revealing the galactose to be bound to the 4-position of GlcNAc. The PA-trisaccharide ***12***-Fuc-Gal appears identical to the PA-trisaccharides ***8-5*** and ***10-2***-Gal (Tables IV, V). By these analyzes, the structural element Galβ4[Fucα3]GlcNAc (Le^x-trisaccharide) was shown to be present in the PA-pentasaccharide ***12***. This coincided with the recognition of CPH by the anti-CD15 mAb G8G12. When compared with the Le^x-PA-pentasaccharide ***12***, the PA-hexasaccharide ***13-2*** contained an additional fucose and the galactose was no longer terminal, but 3-substituted. Enzymatic removal of one Fuc-residue yielded ***13-2***-Fuc, which contained a terminal galactose and thus indicated the fucose to be 3-linked to the galactose. ***13-2***-Fuc was identical to the Le^x-PA-pentasaccharide ***12*** (Tables IV, V). This revealed the PA-hexasaccharide ***13-2***, with its structural element Fucα3Galβ4[Fucα3]GlcNAc-, as a structural isomer of the Lewis Y (Le^y) epitope Fucα2Galβ4[Fucα3]GlcNAc-, with the second Fuc-residue of the former bound to galactose in the 3-position instead of the 2-position. The PA-hexasaccharide ***13-2*** was, therefore, termed pseudo-Le^y. A second PA-hexasaccharide (***14-3***) differed from the PA-pentasaccharide ***12*** in the additional presence of a 3-substituted GlcNAc (Table IV). Removal of terminal Fuc led to the conversion of the 3,4-disubstituted GlcNAc to a 4-substituted GlcNAc (***14-3***-Fuc) which showed the Fuc-residue to be 3-linked to the disubstituted GlcNAc. If we also assume ***14-3*** to be based on the schisto-core structure, as confirmed by the PA-derivatized di-, tri-, tetra- and pentasaccharides analyzed in this study, then these data would not differentiate between the alternative structures Gal4[Fuc3]GlcNAc3GlcNAc3GalNAc4Glc-PA and Gal3GlcNAc4[Fuc3]GlcNAc3GalNAc4Glc-PA. Removal of the terminal Gal, however, led to the conversion of the 4-substituted GlcNAc to a terminal residue, leaving the 3-substituted GlcNAc unchanged (Table IV), and yielding the PA-tetrasaccharide ***14-3***-Fuc-Gal. Hence, these data support the linear sequence Galβ4GlcNAcβ3GlcNAcβ3GalNAcβ4Glc-PA for ***14-3***-Fuc. The PA-tetrasaccharide ***14-3***-Fuc-Gal differs from the PA-trisaccharides ***8-5***, ***10-2***-Gal, and ***12***-Fuc-Gal only in the 3-substituted GlcNAc increment. As with PA-pentasaccharide ***12***, cleavage by α-fucosidase and β-galactosidase associated with linkage analysis has shown the Le^x-structure to be present in ***14-3*** (Tables IV and V) and, therefore, allowed the structure of ***14-3*** to be defined as Galβ4[Fucα3]GlcNAc3GlcNAc3GalNAc4Glc-PA (Le^x-hexasaccharide). For the PA-octasaccharide ***13-3***, two terminal and two subterminal Fuc-residues were found (Table IV). A 20 d-incubation with α-fucosidase removed two of these fucoses (***13-3***-Fuc). The PA-octasaccharide ***13-3*** diverged from the biosynthetic series connecting the other analyzed PA-oligosaccharides in having two 3-linked GalNAc residues. However,

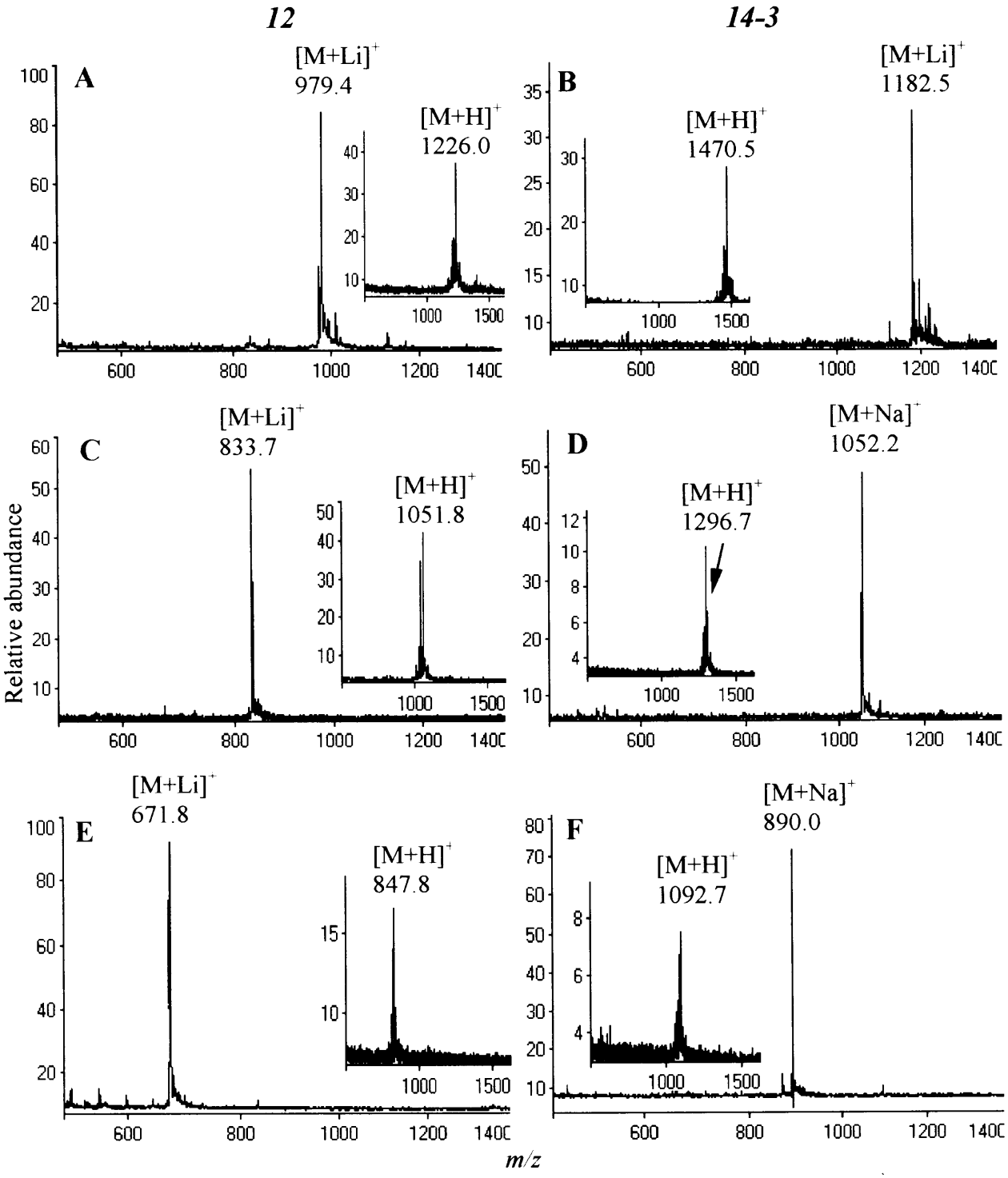

Fig. 5. MALDI-TOF-MS analysis of the PA-pentasaccharide ***12*** and the PA-hexasaccharide ***14-3*** before and after cleavage and HPLC purification. Spectra (**A**–**F**) are of the native PA-oligosaccharides and the inserts of their correspondingly permethylated PA-oligosaccharides. (**A**) PA-pentasaccharide ***12***; (**B**) PA-hexasaccharide ***14-3***; (**C**) ***12*** following combined α-fucosidase and partial acid hydrolysis defucosylation; (**D**) ***14-3*** following α-fucosidase treatment; (**E**) ***12***-Fuc-Gal (***12*** following defucosylation and β-galactosidase treatment); (**F**) ***14-3***-Fuc-Gal (***14-3*** following α-fucosidase and β-galactosidase treatments). All cleavage products were purified by HPLC. Pseudomolecular ions are given in accurate, monoisotopic mass values rounded up to the first decimal place.

the obtained data were insufficient to define its complete structure. For fraction ***16***, the composition of the components deduced from the MALDI-TOF-MS masses (Table II) and from methylation linkage analysis (data not shown) indicated structures with a longer *N*-acetylhexosamine backbone, but due to the complexity and heterogeneity of these latter fractions and the small amounts of material available, the structures could not be defined in detail.

Table IV. Methylation analysis of cercarial glycolipids and glycolipid-derived PA-oligosaccharides

Partially methylated alditol acetate	PA-Oligosaccharide fraction													Glycolipid			Linkage
	6-1	***8-5***	***10-2***	***10-2***-Gal	***12***	***12***-Fuc	***12***-Fuc-Gal	***13-2***	***13-2***-Fuc	***13-3***	***14-3***	***14-3***-Fuc	***14-3***-Fuc-Gal	CDH	CPH	Le^xD	
2,3,4-FucOH		(0.4)	(0.1)		1.0			1.5	0.6	2.0	1.3				1.0	0.7	Fuc(1-
3,4-FucOH										1.6							-2)Fuc(1-
2,3,4,6-GalOH		(0.3)	1.2		1.1	0.6			1.0		1.0	0.7			0.9	1.0	Gal(1-
2,4,6GalOH								1.0								1.4	-3(Gal(1-
2,3,4GalOH								0.1									-6(Gal(1-
2,3,6-GlcOH	*	*	*				*	*	*				*	1.0	1.1		-4)Glc(1-
3,4,6-GlcN(Me)AcOH		1.0		1.0			1.0						1.0				GlcNAc(1-
3,4,6-GalN(Me)AcOH	1.0													+			GalNAc(1-
4,6-GlcN(Me)AcOH											0.9	0.8	1.1				-3)GlcNAc(1-
3,6-GlcN(Me)AcOH			0.8			1.0						1.2					-4)GlcNAc(1-
4,6-GalN(Me)AcOH		0.9	1.0	1.25	1.0	1.0	0.4	+	0.4	1.1	0.8	1.0	0.9		+		-3)GalNAc(1-
6-GlcN(Me)AcOH		(0.2)	(0.3)		0.8			+	0.35	0.5	0.7				+	+	-3,4)GlcNAc(1-

Partially methylated alditol acetates were analyzed by GC/MS. Results are expressed as relative peak ratios of the alditol acetates found; terminal Gal or Gal(1- as linkage correspond to 2,3,4,6-GalOH, 2,3,4,6-tetra-*O*-methylgalactitol as alditol acetate, etc.; 3-substituted GlcNAc or –3)GlcNAc(1- as linkage correspond to 4,6-GlcN(Me)AcOH, 2-deoxy-2-(*N*-methyl)acetamido-4,6-di-*O*-methylglucitol as alditol acetate, etc. Substoichometric amounts of hexosamine species are indicated by (+) and glucose contaminations are marked by an asterisk (*). The partially methylated alditol acetates given in parentheses are due to the presence of the Le^x-PA-pentasaccharide ***12*** as a minor contaminant in ***8-5*** and ***10-2***.

Table V. Defined structures of *S.mansoni* cercarial glycolipid-derived PA-oligosaccharides and their corresponding HPLC-derived fractions

PA-Oligosaccharide structure	Fraction
GalNAc(β1–4)Glc-PA	***6-1***
GlcNAc(β1–3)GalNAc(β1–4)Glc-PA	***8-5***
Gal(β1–4)GlcNAc(β1–3)GalNAc(β1–4)Glc-PA	***10-2***
Gal(β1–4)[Fuc(α1–3)]GlcNAc(β1–3)GalNAc(β1–4)Glc-PA	***12***
Fuc(α1–3)Gal(β1–4)[Fuc(α1–3)]GlcNAc(β1–3)GalNAc(β1–4)Glc-PA	***13-2***
Gal(β1–4)[Fuc(α1–3)]GlcNAc(β1–3)GlcNAc(β1–3)GalNAc(β1–4)Glc-PA	***14-3***

On-target enzymatic cleavage

In order to determine the anomeric configuration of the *N*-acetylhexosamine backbone linkages, PA-oligosaccharides were cleaved on-target with β-*N*-acetylhexosaminidases. The PA-disaccharide ***6-1*** could be cleaved by bovine kidney β-*N*-acetylhexosaminidase. The cleavage product was a PA-monosaccharide, which was observed by MALDI-TOF-MS in its protonated form (259.2 Da; Figure 6D). The pseudomolecular ion at *m/z* 259 did not occur in the PA-disaccharide sample (Figure 6A, insert) or in the enzyme control lacking substrate PA-oligosaccharide (Figure 6G, insert). Though the product PA-monosaccharide signal is located in the matrix ion region of the spectrum, the major ion at *m/z* 259.2 in Figure 6D, together with the control measurements in Figure 6A and G, clearly documented that the PA-disaccharide was cleaved by the β-*N*-acetylhexosaminidase applied. The PA-trisaccharide ***8-5*** ($[M+Li]^+$ 671.3 Da) was analyzed in the same way and resulted in product ions of the same mass ($[M+H]^+$ 259.3 Da). This indicated that both the terminal GlcNAc and the subterminal, 3-substituted GalNAc (Table IV) were β-linked, with the resulting structure for ***8-5*** of GlcNAcβ3GalNAcβ4Glc-PA (Table V). For ***10-2***-Gal, which is a PA-trisaccharide with the same mass (Table II) and linkages (Table IV) as ***8-5***, on-target cleavage with bovine kidney β-*N*-acetylhexosaminidase resulted again in a pseudomolecular ion at *m/z* 259, so that its structure was identical to the PA-trisaccharide ***8-5*** (data not shown). The PA-trisaccharide ***12***-Fuc-Gal was converted following on-target cleavage from the PA-trisaccharide lithium-adduct (671.8 Da; Figure 6B) to the protonated PA-monosaccharide (259.2 Da; Figure 6E, insert). Together with the linkage data (Table IV), ***12***-Fuc-Gal could be assigned the structure GlcNAcβ3GalNAcβ4Glc-PA, which is identical to ***8-5*** and ***10-2***-Gal. Also, in the PA-tetrasaccharide ***14-3***-Fuc-Gal, all linkages could be cleaved by β-*N*-acetylhexosaminidase, as was shown by the observed protonated PA-monosaccharide product (Figure 6F and inset). Together with the linkage data (Table IV), the proposed structure was GlcNAcβ3GlcNAcβ3GalNAcβ4Glc-PA. All these on-target enzymatic cleavage experiments were also performed with the β-*N*-acetylhexosaminidases of *Diplococcus pneumoniae* and jack bean. Like the bovine kidney enzyme, both these enzymes were able to cleave the PA-oligosaccharides ***6-1***, ***8-5***, ***10-2***-Gal, ***12***-Fuc-Gal, and ***14-3***-Fuc-Gal in a 150 min on-target cleavage experiment (data not shown). While the jack bean enzyme was approximately as efficient as the bovine kidney β-*N*-acetylhexosaminidase, cleavage with the *D.pneumoniae* enzyme was less complete, due to the reduced amount of enzyme applied (see *Materials and methods*: On-target

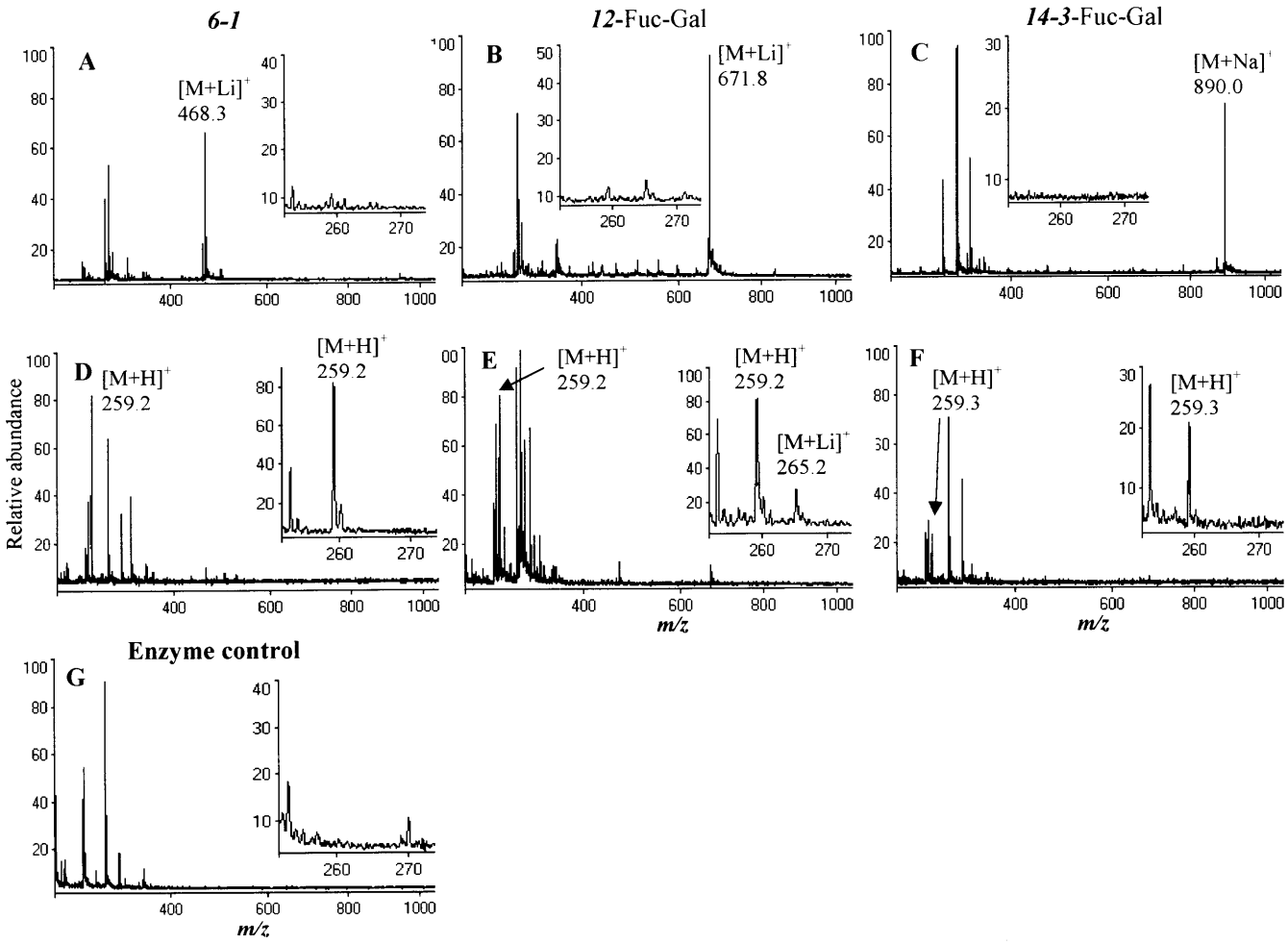

Fig. 6. On-target enzymatic cleavage and MALDI-TOF-MS analysis of the PA-disaccharide ***6-1***, PA-trisaccharide ***12***-Fuc-Gal and PA-tetrasaccharide ***14-3***-Fuc-Gal. The native PA-oligosaccharides ***6-1*** (**A**), ***12***-Fuc-Gal (**B**) and ***14-3***-Fuc-Gal (**C**) were measured by MALDI-TOF-MS. The sample spots were incubated with β-*N*-acetylhexosaminidase from bovine kidney for 150 min and remeasured (**D**, ***6-1***; **E**, ***12***-Fuc-Gal; **F**, ***14-3***-Fuc-Gal). When the enzyme was incubated without substrate (**G**), the resulting mass spectrum did not show signals interfering with the 259 Da cleavage products observed (**D**–**G**). Pseudomolecular ions are given in accurate, monoisotopic mass values rounded up to the first decimal place.

enzymatic cleavage). The latter treatment yielded pseudomolecular ions of the parent compound and the final cleavage product Glc-PA (*m/z* 259). Only ***8-5*** generated significant pseudomolecular ions of the intermediate cleavage product GalNAcβ4Glc-PA, in addition to, Glc-PA as the dominant product.

The structures of the PA-oligosaccharides determined in this study are listed in Table V. Besides the novel Le^x and pseudo-Le^y structures found in *S.mansoni* cercariae, glycolipids similar to those found in eggs (Khoo *et al.*, 1997) were also represented in the cercarial life-cycle stage, as indicated by 2-substituted fucose in methylation analysis (Figure 2) and the data obtained for the PA-octasaccharide ***13-3*** (Table IV).

Discussion

In this study, the structures of complex, antigenic glycolipids from *S.mansoni* have been analyzed. It represents the first investigation on cercarial stage complex glycolipids, as the two previous reports have been on the structural analysis of egg stage glycolipids (Levery *et al.*, 1992; Khoo *et al.*, 1997). Our work has shown *S.mansoni* complex glycolipids from cercariae to differ significantly from egg stage glycolipids in containing large amounts of terminal and 3-substituted galactose. Since galactose was not found in egg glycolipids (Khoo *et al.*, 1997), our study reveals stage-dependent differences with regard to the presence of Le^x-structures in cercarial and absence from egg glycolipids. The carbohydrate moiety was cleaved from the ceramide enzymatically with a high efficacy by *Rhodococcus sp.* endoglycoceramidase II. This enzyme has been shown to be active on glycosphingolipids of the ganglio-, globo- and lacto-series, all of which have the core structure -Galβ4Glcβ1Cer, but not on gala-series glycosphingolipids, cerebrosides or sulfatides (Ito and Yamagata, 1989).

For enzymatic digestion of PA-oligosaccharides, besides the conventional incubation in solution, on-target cleavage was performed in the presence of a 6-aza-2-thiothymine matrix, which allowed the anomeric configuration determination of the

N-acetylhexosamine backbone with minimal sample consumption (Geyer *et al.*, 1999).

While the surface of *S.mansoni* cercariae reacts with an anti-Le^x-mAb only at the acetabular gland opening, the Le^x epitope is expressed in patches over the whole surface of the parasite after transformation (Köster and Strand, 1994). We have identified glycolipid-bound Le^x in the cercarial stage (Table V). It is not yet clear, however, whether lipid- and/or protein-bound glycoconjugates are responsible for the surface-located expression of this epitope after transformation. Its presence at the surface of the schistosome blood fluke conforms with the concept of molecular mimicry, as Le^x is expressed in a wide range of mouse and human tissues (Fox *et al.*, 1983) and is thus an autoantigen. Human granulocytes have Le^x-, often in parallel with sialyl-Le^x-integrated glycoproteins (Fukuda *et al.*, 1984; Spooncer *et al.*, 1984) and glycolipids (Fukuda *et al.*, 1985; Symington *et al.*, 1985). The epitope has been shown to interact homophilically in cellular adhesion (Eggens *et al.*, 1989) and has been structurally identified on the *N*-glycans of leukocyte cell adhesion molecules (Asada *et al.*, 1991). As this epitope is shared by the parasite and its definitive host, an anti-Le^x immune response occurred during schistosome infection (Nyame *et al.*, 1995, 1996, 1997) and putatively caused complement-dependent lysis of host neutrophils; high anti-Le^x antibody titers were correlated with the severity of the resultant neutropenia (Borojevic *et al.*, 1983).

Besides the Le^x and pseudo-Le^y structures found in *S.mansoni* cercariae for the first time (Table V), glycolipids similar to those found in eggs (Khoo *et al.*, 1997) were also present in the cercarial life-cycle stage in amounts that did not allow detailed structural analysis. The high amount of 2-substituted Fuc revealed by methylation analysis of the cercarial complex glycolipid fraction could not be substantiated by the PA-oligosaccharides analyzed, except for ***13-3*** (Table IV). Some 2-substituted fucose could be present in the fractions ***15*** to ***17***, but they have not been analyzed further due to their heterogeneity and lack of material. Glycosphingolipid biosynthesis in cercariae appears to differ significantly from that in eggs (Khoo *et al.*, 1997), as deduced from the structures detected. There are different structures present in the *N*-acetylhexosamine backbone. In the egg stage, the chain is built up with repeating units of –4GlcNAcβ- linked to the schisto-core structure, –3GalNAcβ4Glc1Cer, and GalNAcβ- serves as a termination signal for the *N*-acetylhexosamine backbone (Khoo *et al.*, 1997). The cercarial Le^x ceramide hexahexoside (corresponding to the ***14-3*** PA-hexasaccharide; Table V) was found to have a GlcNAcβ3GlcNAc linkage, not previously described in schistosomes, in contrast to egg stage glycosphingolipids with their dominant GlcNAcβ4GlcNAc linkages (Khoo *et al.*, 1997). This was paralleled by the presence of the 3-substituted *N*-acetylglucosamine in the cercarial complex glycolipid fraction and PA-oligosaccharide fraction ***16*** (cf. Figure 2 and Table IV) and its absence from egg complex glycolipids (Khoo *et al.*, 1997). Schistosome β4- or β3-*N*-acetylglucosaminyltransferases have not yet been described, but for the snail host *Lymnea stagnalis* of the bird schistosome *Trichobilharzia ocellata* one of these enzymes has been cloned and characterized (Bakker *et al.*, 1994), which was shown to transfer GlcNAc to GlcNAcβ- to yield the chitobiose structure GlcNAcβ4GlcNAcβ-. Besides the different *N*-acetylhexosamine backbones, egg and cercarial glycolipids demonstrate differences in the degree of galactosylation: while egg glycosphingolipids lack galactose, our structural data would indicate a β4-galactosyltransferase to act on the terminal *N*-acetylglucosamine of the glycosphingolipid *N*-acetylhexosamine backbone. A β4-galactosyltransferase activity has been measured in extracts from adult worms and found to be able to synthesize *N*-acetyllactosamine structures (Rivera-Marrero and Cummings, 1990). This enzyme activity could be involved in the galactosylation of circulating cathodic antigen in the adult worm and, also, hypothetically in the biosynthetic pathway of the cercarial glycolipids. Galactosylation may be accompanied by fucosylation to yield the Le^x structures. An α3-fucosyltransferase activity has been detected in extracts of adult *S.mansoni* worms (DeBose-Boyd *et al.*, 1996) and shown to act on *N*-acetyllactosamine to yield Le^x. In addition, a *S.mansoni* fucosyltransferase highly homologous to mouse and human fucosyltransferase VII has been cloned and characterized, but a physiological substrate of this enzyme has not yet been identified (Marques *et al.*, 1998). In cercarial homogenates of the bird schistosome *T. ocellata*, an α3-fucosyltransferase was detected (Hokke *et al.*, 1998) and was found to be active on the GlcNAc of *N*-acetyllactosamine and GalNAcβ4GlcNAcβ- (LacdiNAc). An α2-fucosyltransferase activity has also been described (Hokke *et al.*, 1998), which is thought to be responsible for the synthesis of oligofucosyl side-chains (Khoo *et al.*, 1995, 1997; Hokke *et al.*, 1998). A schistosomal fucosyltransferase acting on the GalNAc of LacdiNAc structures has not yet been identified. This yet to be identified enzyme is a candidate for the synthesis of the pseudo-Le^y structure found in our study. We would assume this enzyme to have a side-activity which would allow it to transfer fucose to the 3-position of both GalNAc and Gal.

Materials and methods

Parasite material

A Puerto Rican isolate of *S.mansoni* was maintained by passage through random-bred mice and *Biomphalaria glabrata* snails. The large-scale production of cercariae from patent snails was performed as described previously (Doenhoff *et al.*, 1981). Infection of 8- to 12-week-old mice was performed percutaneously (Smithers and Terry, 1965). Adult worms were obtained by perfusion ~6 weeks after infection (Doenhoff *et al.*, 1978) and rinsed with perfusion fluid to remove red blood cells. The last resuspension was in deionized water. Parasite eggs were isolated from homogenized, trypsin-digested livers of infected, hydrocortisone acetate (2.5 mg/mouse) treated mice (Doenhoff *et al.*, 1981). Parasite material was freeze-dried and stored at –20°C.

Isolation and purification of complex, neutral glycolipids

Glycolipids were isolated by consecutive extractions using approximately 100 ml of organic solvent per gram dry weight of parasite material: extraction was performed twice with chloroform:methanol:water (10:10:1, by volume) with sonication of the suspension (Branson sonifier B15; Branson, Danbury, CT) for 30 min and incubation at 50°C for 30 min; once with chloroform:methanol:0.8 M aqueous sodium acetate (30:60:8, by volume) with a 30 min sonication step and over-

night incubation at 4°C; and twice with 2-propanol:n-hexane:water (55:20:25, by volume), followed by a 30 min sonication step and 30 min incubation at 50°C. After each extraction step, the sample was centrifuged at 10,000 × *g* for 10 min and the resultant supernatant rotary evaporated to dryness. Raw extracts were mildly saponified using methanolic 0.1 M sodium hydroxide for 2 h at 37°C. Salt and hydrophilic contaminants were removed by reverse-phase chromatography (Chromabond $C18_{ec}$, Macherey and Nagel, Düren, Germany) as described elsewhere (Dennis *et al.*, 1996). The preparation was then dissolved in chloroform:methanol:water (30:60:8, by volume) and applied to a QAE-Sephadex column (10 × 80 mm, acetate form; Pharmacia, Freiburg, Germany), as described elsewhere (Itonori *et al.*, 1991). Briefly, the neutral glycolipid fraction was collected as the flow-through with 50 ml of chloroform:methanol:water (30:60:8, by volume), and the acidic lipid fraction was eluted with 50 ml 0.45 M ammonium acetate in methanol. The neutral fraction glycolipids were purified by Florisil chromatography (Dennis *et al.*, 1998), resolved on a silica-gel cartridge (Waters, Eschborn, Germany; Dennis *et al.*, 1995) and analyzed by HPTLC and orcinol/H_2SO_4-staining, as well as HPTLC-immunostaining. CMH/CDH and complex, neutral glycolipids were separated into two pools.

HPTLC

For HPTLC, the complex, neutral glycolipids were separated on silica-gel 60 plates (Merck, Darmstadt, Germany) with chloroform:methanol: 0.25% KCl (50:40:10, by volume) as the developing solvent in an automatic HPTLC-developing tank (DC-MAT; Baron, Reichenau, Germany). Glycosphingolipids were visualized chemically by orcinol/H_2SO_4-staining (Dennis *et al.*, 1998) or, alternatively, by immunostaining (Baumeister *et al.*, 1994). The globoside standard was purchased from ICT (Bad Homburg, Germany). A Le^x-neoglycolipid (Le^xD) was used as a positive control in immunostaining and was prepared according to the literature (Feizi *et al.*, 1994) by reductive amination of lacto-*N*-fucopentaose III (Dextra Laboratories, Reading, England) with dihexadecanoyl-L-α-phosphatidyl-ethanolamine (Sigma, Deisenhofen, Germany). For immunostaining, the developed HPTLC plates were coated with polyisobutylmethacrylate (Plexigum P28; Aldrich, Steinheim, Germany), blocked with bovine serum albumin–containing phosphate-buffered saline and incubated with the primary antibody for at least 2 h at room temperature. The primary antibodies used were: sera from 8 mice with chronic *S.mansoni* infection (CIS1-8); mouse-mAb anti-CD15 BRA4F1 (Biogenex, San Ramon, CA; IgM, recognizing the Le^x-epitope); mouse-mAb anti-CD15 4D1 (IgM; kindly provided by Dr. B.Kniep); mouse-mAb G8G12 (kindly provided by Dr. Q.Bickle; generated in a CBA mouse against irradiated cercariae followed by a booster against non-irradiated cercariae prior to fusion of the spleen cells; Bickle *et al.*, 1986). Horseradish peroxidase-coupled, rabbit anti-mouse Ig (Dako Diagnostics, Hamburg, Germany) was used as secondary antibody. As a modification to the described method (Baumeister *et al.*, 1994), following secondary antibody incubation the plate was washed twice with phosphate-buffered saline and equilibrated once (5 min) with sodium citrate buffer (100 mM, pH 6.0). For staining, 240 µl of a substrate stock solution (97.5 mg of chloronaphthol (Sigma) and 60 mg diethylphenylenediamine (Sigma) in a mixture of 9 ml acetonitrile and 1 ml methanol, and stored at –20°C) and 8 µl of 30% H_2O_2 (Merck) were added to 10 ml of sodium citrate buffer. The plate was overlaid with this substrate solution and bound secondary antibody was visualized by a blue precipitate (Conyers and Kidwell, 1991). Alternatively, alkaline phosphatase–coupled, goat anti-mouse Ig (Sigma) was applied as secondary antibody (Bethke *et al.*, 1986; Müthing, 1998) and binding visualized by use of 10 mg of 5-bromo-4-chloro-3-indolyl phosphate (Biomol, Hamburg, Germany) and 5 mg nitro-blue tetrazolium chloride (Sigma) as substrates in 10 ml glycine buffer, 100 mM, pH 10.4, containing 1 mM $ZnCl_2$ and 1 mM $MgCl_2$.

Preparation of CDH and CPH

For the isolation of individual glycosphingolipids, HPLC fractionation on a porous silica gel column (Iatrobeads 6RS-8010, 10 µm, 4.6 × 500 mm; Macherey and Nagel) at a flow rate of 1 ml/min was performed. The column was equilibrated with 2% methanol in chloroform (by volume) and the sample was dissolved in chloroform:methanol (9:1, v/v). After injection, the column was run isocratically for 15 min, then within a further 60 min period the methanol content of the eluting solvent was increased to 38% (by volume). The column was washed with methanol.

Preparation of PA-oligosaccharides

Aliquots of the cercarial, complex, neutral glycolipid fraction were dissolved in 200 µl 50 mM sodium acetate buffer (pH 5.0; 0.1% sodium taurodeoxycholate), sonicated for 5 min at 50°C. Recombinant endoglycoceramidase II (20 µl (40 mU); from *Escherichia coli* encoding the gene of *Rhodococcus sp.* endoglycoceramidase II; Takara Shuzu Co., Ltd., Otsu, Shiga, Japan) was added, the sample incubated at 37°C for 72 h and 20 mU of fresh enzyme added each day. Samples were applied to a RP-cartridge (500 mg; Chromabond $C18_{ec}$, Macherey and Nagel), washed with 10 ml of water to obtain the released oligosaccharides, and uncleaved glycolipids and free ceramides were eluted with 10 ml methanol and 20 ml chloroform:methanol (2:1, v/v). Washes and eluates were lyophilized or rotary evaporated to dryness, and released oligosaccharides as well as uncleaved glycolipids were quantitated by carbohydrate composition analysis. Coupling reagent (20 µl; 200 mg sublimation-purified 2-aminopyridine in 53 µl glacial acetic acid) was added to the dry, released oligosaccharides (Natsuka and Hase, 1998). After incubation at 90°C for 60 min, 70 µl of the reduction reagent were added (200 mg dimethylamine-borane complex in 50 µl water and 80 µl acetic acid) and incubated at 80°C for 35 min. Samples were adjusted to pH 10 by addition of NH_3 (25% in water) and the volume was adjusted to 400 µl by addition of water. The reaction mixture was extracted six times with 600 µl chloroform to reduce the 2-aminopyridine excess and the 2-aminopyridine-labeled oligosaccharides (PA-oligosaccharides) were lyophilized.

Amino-phase-HPLC

PA-oligosaccharides were fractionated on an amino-phase HPLC column (4.6 × 250 mm, Nucleosil-Carbohydrate; Macherey and Nagel) at a flow rate of 1 ml/min at room temperature (RT) and detected by fluorescence (310/380 nm). The column was equilibrated with 200 mM aqueous triethylamine-acetic acid, pH 7.3: acetonitrile (25%:75%). A gradient

of 25–60% aqueous triethylamine-acetic acid buffer was applied within a 60 min period and the column was run isocratically for a further 10 min. Fractions of 2 ml were collected and lyophilized.

RP-HPLC

PA-oligosaccharides were fractionated on a RP-HPLC column (C_{18}, 4.6 × 250 mm; Hypersil, Astmoor, Runcorn, Cheshire, UK) at a flow rate of 0.8 ml/min at RT and detected by fluorescence (320/400 nm). The column was equilibrated with aqueous 0.01% trifluoroacetic acid. A gradient from 0 to 3% acetonitrile in a period of 150 min was applied. Fractions of 1.6 ml were collected and lyophilized.

MALDI-TOF-MS

For MALDI-TOF-MS-experiments, the 6-aza-2-thiothymine matrix (Sigma) was spotted at 0.5 µl (5 mg/ml in water) onto the stainless-steel target. Approximately 1 µl of the PA-oligosaccharides dissolved in water was added to the matrix droplet and dried in a gentle stream of cold air. Glycolipids were dissolved in chloroform:methanol:water (10:10:1, by volume), and 1 µl was added to a dry matrix spot under a stream of warm air. MALDI-TOF-MS was performed on a Vision 2000 time-of-flight mass spectrometer (Finningan/MAT, Bremen, Germany) equipped with a UV-nitrogen laser (337 nm). The instrument was operated in the positive-ion reflectron mode throughout. All spectra represent accumulated spectra obtained by 3–20 laser shots and given molecular masses represent the monoisotopic masses rounded up to the first decimal place. The instrument was calibrated with the monoisotopic peak of angiotensin I (Sigma) and a matrix peak (285.0 Da).

On-target enzymatic cleavage

PA-oligosaccharide samples applied to the MALDI-TOF-MS-target were first used to determine the molecular mass of the intact molecule. Then the same sample spot was analyzed by on-target exoglycosidase treatment and subsequent MALDI-TOF-MS measurement of the cleavage product (Geyer *et al.*, 1999). For this, the sample was redissolved in 2 µl of dialyzed enzyme solution. The target was placed in a screw-capped jar containing ammonium acetate buffer at the bottom and incubated at 37°C for 150 min. Subsequently, spots were dried in a cold stream of air and the mass profile of the digestion products was recorded. The enzymes used were β-*N*-acetylhexosaminidase from jack bean (133 mU/µl; Sigma), from bovine kidney (50 mU/µl; Boehringer Mannheim, Mannheim, Germany), and from *D.pneumoniae* (1 mU/µl; Boehringer Mannheim). All enzymes were dialyzed for 4 h against 25 mM ammonium acetate buffer adjusted to the optimal pH for each enzyme (pH 4.5 for the bovine kidney enzyme and pH 5.0 for the *D.pneumoniae* and jack bean enzymes). The dialyzed enzymes were used undiluted for on-target cleavage.

Exoglycosidase treatment

PA-oligosaccharides were treated with either α-fucosidase from bovine kidney (4 mU/µl; Boehringer Mannheim) or with β-galactosidase from *E.coli* (500 mU/µl; Sigma). Enzymes were dialyzed for 4 h against 25 mM ammonium acetate solution adjusted to the optimal pH for each enzyme (pH 5.0 for α-fucosidase and pH 7.3 for β-galactosidase). The dialyzed enzymes (50 µl) were added undiluted to the dried PA-oligosaccharides and the sample was incubated at 37°C. When incubation was continued for more than 24 h, 20 µl of dialyzed enzyme was added to the sample each day. The PA-oligosaccharide ***13-3*** was incubated with dialyzed α-fucosidase for 20 days in the presence of 0.02% sodium azide in order to inhibit microbial growth, and fresh enzyme was added each week. Following enzymatic cleavage, the PA-oligosaccharides were analyzed for their characteristic pseudomolecular ions by MALDI-TOF-MS.

Partial acid hydrolysis

For partial hydrolysis (Khoo *et al.*, 1995), complex, neutral glycolipids were incubated in 100 µl of TFA-solution (0.1–0.2 M) at 80°C for 40–80 min, and the resultant samples were dried down in a Speed-Vac.

Monosaccharide composition analysis

For composition analysis, samples were hydrolyzed in 100 µl 4 N aqueous TFA (Merck) at 100°C for 4 h, and dried down in a Speed-Vac. For derivatization with anthranilic acid (Anumula, 1994), the samples were dissolved in 10 µl 0.6% sodium acetate solution with sonication. The reagent solution was obtained by dissolving 6 mg anthranilic acid (Sigma) and 20 mg sodium cyanoborohydride (Sigma) in 1 ml methanol containing 2.4% sodium acetate and 2% boric acid, 50 µl of which was added to the sample. After a 45 min incubation at 80°C, the derivatized monosaccharides were resolved by HPLC and detected by fluorescence (360/425 nm) after separation on a Superspher RP 18ec column (4 µm, 4 × 250 mm; Merck) at a flow rate of 1 ml/min. The column was equilibrated in aqueous 0.2% 1-butylamine, 0.5% phosphoric acid and 1% tetrahydrofuran (by volume) containing 2.5% acetonitrile. After injection, the column was run isocratically for 5 min, then within 17 min the acetonitrile content was raised to 9% and followed by a final 15 min wash step at 50% acetonitrile.

Methylation-linkage analysis

PA-oligosaccharides and glycolipids were permethylated (Paz-Parente *et al.*, 1985) and hydrolyzed (4 N aqueous TFA, 100°C, 4 h). Partially methylated alditol acetates obtained after sodium borohydride reduction and peracetylation were analyzed by capillary GC/MS, using the instrumentation and microtechniques described elsewhere (Geyer and Geyer, 1994). Lacto-*N*-tetraose was used as a standard for the identification of 4,6-GlcN(Me)AcOH.

Acknowledgments

We acknowledge the expert technical assistance of Markus Schwinn, Peter Kaese, Werner Mink, and Siegfried Kühnhardt. The authors wish to thank Dr. Bernhard Kniep, Institute of Immunology, Technical University-Dresden, Germany, for provision of the mAb anti-Le^x 4D1, and Dr. Quentin Bickle, Department of Infectious and Tropical Diseases, London School of Hygiene and Tropical Medicine, England, for supply of the mAb G8G12. This study was supported by the German Research Council (SFB 535, Teilprojekt Z1 and Graduier-

tenkolleg “Molecular Biology and Pharmacology”). This paper is in partial fulfilment of the requirements of M.Wuhrer for the degree of Dr. rer. nat. at Giessen University.

Abbreviations

CIS, chronic infection serum; CDH, ceramide dihexoside; CMH, ceramide monohexoside; CPH, ceramide pentahexoside; Fuc; fucose; GC/MS, gas chromatography/mass spectrometry; Gal, galactose; GalNAc, *N*-acetylgalactosamine; Glc, glucose; GlcNAc, *N*-acetylglucosamine; HPLC, high-performance liquid chromatography; HPTLC, high-performance thin-layer chromatography; Le^x, Lewis X; Le^xD, Le^x-dihexadecanoyl-α-L-phosphatidylethanolamine neoglycolipid; Le^y, Lewis Y; mAb, monoclonal antibody; MALDI-TOF-MS, matrix-assisted laser desorption/ionization time-of-flight mass spectrometry; Man, mannose; RP-cartridge, reverse-phase cartridge; RT, room temperature; TFA, trifluoroacetic acid.

References

Anumula,K.R. (1994) Quantitative determination of monosaccharides in glycoproteins by high-performance liquid chromatography with highly sensitive fluorescence detection. *Anal. Biochem.*, **220**, 275–283.

Asada,M., Furukawa,K., Kantor,C., Gahmberg,C.G. and Kobata,A. (1991) Structural study of the sugar chains of human leukocyte cell adhesion molecules CD11/CD18. *Biochemistry*, **30**, 1561–1571.

Bakker,H., Agterberg,M., van Tetering,A., Koeleman,C.A., van den Eijnden,D.H. and van Die,I. (1994) A *Lymnaea stagnalis* gene, with sequence similarity to that of mammalian β1–4-galactosyltransferases, encodes a novel UDP-GlcNAc:GlcNAcβ-R β1-4-*N*-acetylglucosaminyltransferase. *J. Biol. Chem.*, **269**, 30326–30333.

Baumeister,S., Dennis,R.D., Klunder,R., Schares,G., Zahner,H. and Geyer,E. (1994) *Litomosoides carinii*: macrofilariae-derived glycolipids—chromatography, serology and potential in the evaluation of anthelminthic efficacy. *Parasite Immunol.*, **16**, 629–641.

Bergwerff,A.A., van Dam,G.J., Rotmans,J.P., Deelder,A.M., Kamerling,J.P. and Vliegenthart,J.F.G. (1994) The immunologically reactive part of immunopurified circulating anodic antigen from *Schistosoma mansoni* is a threonine-linked polysaccharide consisting of –6)- (β-D-Glc*p*A- (1–3))-β-D-Gal*p*NAc- (1- repeating units. *J. Biol. Chem.*, **269**, 31510–31517.

Bethke,U., Müthing,J., Schauder,B., Conradt,P. and Mühlradt,P.F. (1986) An improved semi-quantitative enzyme immunostaining procedure for glycosphingolipid antigens on high performance thin layer chromatograms. *J. Immunol. Methods*, **89**, 111–116.

Bickle,Q.D., Andrews,B.J. and Taylor,M.G. (1986) *Schistosoma mansoni*: characterization of two protective monoclonal antibodies. *Parasite Immunol.*, **8**, 95–107.

Borojevic,R., Santos-da-Silva,C. and Carvalho,E.A. (1983) Chronic schistosomiasis mansoni: splenic myelopoiesis and inhibition of neutrophil granulocytopoiesis mediated by the sera of patients. *J. Infect. Dis.*, **148**, 422–426.

Conyers,S.M. and Kidwell,D.A. (1991) Chromogenic substrates for horseradish peroxidase. *Anal. Biochem.*, **192**, 207–211.

Cummings,R.D. and Nyame,A.K. (1996) Glycobiology of schistosomiasis. *FASEB J.*, **10**, 838–848.

Dalton,J.P., Lewis,S.A., Aronstein,W.S. and Strand,M. (1987) *Schistosoma mansoni*: immunogenic glycoproteins of the cercarial glycocalyx. *Exp. Parasitol.*, **63**, 215–226.

DeBose-Boyd,R., Nyame,A.K. and Cummings,R.D. (1996) *Schistosoma mansoni*: characterization of an α1-3 fucosyltransferase in adult parasites. *Exp. Parasitol.*, **82**, 1–10.

Deelder,A.M. and Kornelis,D. (1980) *Schistosoma mansoni*: characterization of two circulating polysaccharide antigens and the immunological response to these antigens in mouse, hamster and human infections. *Exp. Parasitol.*, **50**, 16–32.

Dennis,R.D., Baumeister,S., Smuda,C., Lochnit,G., Waider,T. and Geyer,E. (1995) Initiation of chemical studies on the immunoreactive glycolipids of adult *Ascaris suum*. *Parasitology*, **110**, 611–623.

Dennis,R.D., Baumeister,S., Lauer,G., Richter,R. and Geyer,E. (1996) Neutral glycolipids of *Schistosoma mansoni* as feasible antigens in the detection of schistosomiasis. *Parasitology*, **112**, 295–307.

Dennis,R.D., Lochnit,G. and Geyer,R. (1998) Strategies for preliminary characterization of novel amphoteric glycosphingolipids. *Methods Mol. Biol.*, **76**, 197–212.

Doenhoff,M.J., Bickle,Q., Long,E., Bain,J. and McGregor,A. (1978) Factors affecting the acquisition of resistance against *Schistosoma mansoni* in the mouse. I. Demonstration of resistance to reinfection using a model system that involves perfusion of mice within three weeks of challenge. *J. Helminthol.*, **52**, 173–186.

Doenhoff,M.J., Pearson,S., Dunne,D.W., Bickle,Q., Lucas,S., Bain,J., Musallam,R. and Hassounah,O. (1981) Immunological control of hepatotoxicity and parasite egg excretion in *Schistosoma mansoni* infections: stage specificity of the reactivity of immune serum in T-cell deprived mice. *Trans. R. Soc. Trop. Med. Hyg.*, **75**, 41–53.

Eggens,I., Fenderson,B., Toyokuni,T., Dean,B., Stroud,M. and Hakomori,S. (1989) Specific interaction between Le^x and Le^x determinants. A possible basis for cell recognition in preimplantation embryos and in embryonal carcinoma cells. *J. Biol. Chem.*, **264**, 9476–9484.

Feizi,T., Stoll,M.S., Yuen,C.-T., Chai,W. and Lawson,A.M. (1994) Neoglycolipids: probes of oligosaccharide structure, antigenicity and function. *Methods Enzymol.*, **230**, 484–519.

Fox,N., Damjanov,I., Knowles,B.B. and Solter,D. (1983) Immunohistochemical localization of the mouse stage-specific embryonic antigen 1 in human tissues and tumors. *Cancer Res.*, **43**, 669–678.

Fukuda,M., Spooncer,E., Oates,J.E., Dell,A. and Klock,J.C. (1984) Structure of sialylated fucosyl lactosaminoglycan isolated from human granulocytes. *J. Biol. Chem.*, **259**, 10925–10935.

Fukuda,M.N., Dell,A., Oates,J.E., Wu,P., Klock,J.C. and Fukuda,M. (1985) Structures of glycosphingolipids isolated from human granulocytes. The presence of a series of linear poly-N-acetyllactosaminylceramide and its significance in glycolipids of whole blood cells. *J. Biol. Chem.*, **260**, 1067–1082.

Geyer,H., Schmitt,S., Wuhrer,M. and Geyer,R. (1999) Structural analysis of glycoconjugates by on-target enzymatic digestion and MALDI-TOF-MS. *Anal. Chem.*, **71**, 476–482.

Geyer,R. and Geyer,H. (1994) Saccharide linkage analysis using methylation and other techniques. *Methods Enzymol.*, **230**, 86–107.

Hellerqvist,C.G. (1990) Linkage analysis using Lindberg method. *Methods Enzymol.*, **193**, 554–573.

Hokke,C.H., Neeleman,A.P., Koeleman,C.A.M. and van den Eijnden,D.H. (1998) Identification of an α3-fucosyltransferase and a novel α2-fucosyltransferase activity in cercariae of the schistosome *Trichobilharzia ocellata*: biosynthesis of the Fucα1-2Fucα1-3[Gal(NAc)β1-4]GlcNAc sequence. *Glycobiology*, **8**, 393–406.

Ito,M. and Yamagata,T. (1989) Purification and characterization of glycosphingolipid-specific endoglycosidases (endoglycoceramidases) from a mutant strain of *Rhodococcus sp.*—evidence for three molecular species of endoglycoceramidase with different specificities. *J. Biol. Chem.*, **264**, 9510–9519.

Itonori,S., Nishizawa,M., Suzuki,M., Inagaki,F., Hori,T. and Sugita,M. (1991) Polar glycosphingolipids in insect: chemical structures of glycosphingolipid series containing 2′-aminoethylphosphoryl-(→6)-N-acetylglucosamine as polar group from larvae of the green-bottle fly, *Lucilia caesar*. *J. Biochem.*, **110**, 479–485.

Khoo,K.H., Sarda,S., Xu,X., Caulfield,J.P., McNeil,M.R., Homans,S.W., Morris,H.R. and Dell,A. (1995) A unique multifucosylated –3GalNAc β1-4GlcNAc β1-3Gal α1- motif constitutes the repeating unit of the complex O-glycans derived from the cercarial glycocalyx of *Schistosoma mansoni*. *J. Biol. Chem.*, **270**, 17114–17123.

Khoo,K.H., Chatterjee,D., Caulfield,J.P., Morris,H.R. and Dell,A. (1997) Structural characterization of glycosphingolipids from the eggs of *Schistosoma mansoni* and *Schistosoma japonicum*. *Glycobiology*, **7**, 653–661.

Ko,A.I., Dräger,U.C. and Harn,D.A. (1990) A Schistosoma mansoni epitope recognized by a protective monoclonal antibody is identical to the stage-specific embryonic antigen 1. *Proc. Natl Acad. Sci. USA*, **87**, 4159–4163.

Köster,B. and Strand,M. (1994) *Schistosoma mansoni*: immunolocalization of two different fucose-containing carbohydrate epitopes. *Parasitology*, **108**, 433–446.

Levery,S.B., Weiss,J.B., Salyan,M.E.K., Roberts,C.E., Hakomori,S., Magnani,J.L. and Strand,M. (1992) Characterization of a series of novel fucose-containing glycosphingolipid immunogens from eggs of *Schistosoma mansoni*. *J. Biol. Chem.*, **267**, 5542–5551.

Makaaru,C.K., Damian,R.T., Smith,D.F. and Cummings,R.D. (1992) The human blood fluke *Schistosoma mansoni* synthesizes a novel type of glycosphingolipid. *J. Biol. Chem.*, **267**, 2251–2257.

Mansour,M.H. (1996) Purification and characterization of SM 37: a fucosyllactose determinant-bearing glycoprotein probed by *Biomphalaria alexandria* lectin on adult male schistosomes. *J. Parasitol.*, **82**, 586–593.

Marques,E.T.A., Weiss,J.B. and Strand,M. (1998) Molecular characterization of a fucosyltransferase encoded by *Schistosoma mansoni*. *Mol. Biochem. Parasitol.*, **93**, 237–250.

Müthing,J. (1998) TLC in structure and recognition studies of glycosphingolipids. *Methods Mol. Biol.*, **76**, 183–195.

Natsuka,S. and Hase,S. (1998) Analysis of N- and O-glycans by pyridylamination. *Methods Mol. Biol.*, **76**, 101–113.

Negm,H.I. (1996) Characterization of fucosyllactose determinant-bearing glycoproteins probed by a *Biomphalaria alexandria* lectin in *Schistosoma mansoni* cercariae. *Dev. Comp. Immunol.*, **20**, 87–96.

Nyame,K., Smith,D.F., Damian,R.T. and Cummings,R.D. (1989) Complex-type asparagine-linked oligosaccharides in glycoproteins synthesized by *Schistosoma mansoni* adult males contain terminal β-linked N-acetylgalactosamine. *J. Biol. Chem.*, **264**, 3235–3243.

Nyame,K., Pilcher,J.B., Tsang,V. and Cummings,R.D. (1995) Infection of monkeys and humans with the helminthic parasite *Schistosoma mansoni* induces autoimmunity to the Lewis x antigen. *Glycoconj. J.*, **12**, 531.

Nyame,A.K., Pilcher,J.B., Tsang,V.C.W. and Cummings,R.D. (1996) *Schistosoma mansoni* infection in humans and primates induces cytolytic antibodies to surface Le^x determinants on myeloid cells. *Exp. Parasitol.*, **82**, 191–200.

Nyame,A.K., Pilcher,J.B., Tsang,V.C.W. and Cummings,R.D. (1997) Rodents infected with *Schistosoma mansoni* produce cytolytic IgG and IgM antibodies to the Lewis x antigen. *Glycobiology*, **7**, 207–215.

Nyame,A.K., Debose-Boyd,R., Long,T.D., Tsang,V.C. and Cummings,R.D. (1998) Expression of Le^x antigen in *Schistosoma japonicum* and *S.haematobium* and immune responses to Le^x in infected animals: lack of Le^x expression in other trematodes and nematodes. *Glycobiology*, **8**, 615–624.

Paz-Parente,J., Cardon,P., Leroy,Y., Montreuil,J., Fournet,B. and Ricard,G. (1985) A convenient method for methylation of glycoprotein glycans in small amounts by using lithium methyl-sulfinyl carbanion. *Carbohydr. Res.*, **141**, 41–47.

Rivera-Marrero,C.A. and Cummings,R.D. (1990) *Schistosoma mansoni* contains a galactosyltransferase activity distinct from that typically found in mammalian cells. *Mol. Biochem. Parasitol.*, **43**, 59–67.

Smithers,S.R. and Terry,R.J. (1965) The infection of laboratory hosts with cercariae of *Schistosoma mansoni* and the recovery of the adult worms. *Parasitology*, **55**, 695–700.

Spooncer,E., Fukuda,M., Klock,J.C., Oates,J.E. and Dell,A. (1984) Isolation and characterization of polyfucosylated lactosaminoglycan from human granulocytes. *J. Biol. Chem.*, **259**, 4792–4801.

Srivatsan,J., Smith,D.F. and Cummings,R.D. (1992a) The human blood fluke *Schistosoma mansoni* synthesizes glycoproteins containing the Lewis x antigen. *J. Biol. Chem.*, **267**, 20196–20203.

Srivatsan,J., Smith,D.F. and Cummings,R.D. (1992b) *Schistosoma mansoni* synthesizes novel biantennary Asn-linked oligosaccharides containing terminal β-linked N-acetylgalactosamine. *Glycobiology*, **2**, 445–452.

Symington,F.W., Hedges,D.L. and Hakomori,S. (1985) Glycolipid antigens of human polymorphonuclear neutrophils and the inducible HL-60 myeloid leukemia line. *J. Immunol.*, **134**, 2498–2506.

Umeda,M., Diego,I. and Marcus,D.M. (1986) The occurrence of anti-3-fucosyllactosamine antibodies and their cross-reactive idiotopes in preimmune and immune mouse sera. *J. Immunol.*, **137**, 3264–3269.

van Dam,G.J., Bergwerff,A.A., Thomas-Oates,J.E., Rotmans,J.P., Kamerling,J.P., Vliegenthart,J.F. and Deelder,A.M. (1994) The immunologically reactive O-linked polysaccharide chains derived from circulating cathodic antigen isolated from the human blood fluke *Schistosoma mansoni* have Lewis x as repeating unit. *Eur. J. Biochem.*, **225**, 467–482.

Weiss,J.B., Magnani,J.L. and Strand,M. (1986) Identification of *Schistosoma mansoni* glycolipids that share immunogenic carbohydrate epitopes with glycoproteins. *J. Immunol.*, **136**, 4275–4282.

Weiss,J.B. and Strand,M. (1985) Characterization of developmentally regulated epitopes of *Schistosoma mansoni* egg glycoprotein antigens. *J. Immunol.*, **135**, 1421–1429.